Available online at www.CivileJournal.org

Civil Engineering Journal

Vol. 6, No. 5, May, 2020

# Investigating the Flow Hydrodynamics in a Compound Channel with Layered Vegetated Floodplains

Muhammad Ahmad [a*], Usman Ghani [a], Naveed Anjum [b], Ghufran Ahmed Pasha [a], Muhammad Kaleem Ullah [c], Afzal Ahmed [a]

[a] *Department of Civil Engineering, University of Engineering and Technology Taxila, Taxila, Pakistan.*

[b] *Department of Civil and Environmental Engineering, Graduate School of Science and Engineering, Saitama University, Saitama, Japan.*

[c] *Department of Civil Engineering, The University of Lahore, Lahore, Pakistan.*

Received 22 December 2019; Accepted 11 April 2020

**Abstract**

In natural rivers, vegetation grows on floodplains, generating complex velocity field within the compound channel. The efficient modelling of the flow hydraulics in a compound channel with vegetated floodplains is necessary to understand and determine the natural processes in rivers and streams. As the three dimensional (3D) flow features are difficult to capture through experimental investigation; therefore, the present numerical study was carried out to investigate the complex 3D flow structures with the vertically layered vegetation placed over the floodplains in a symmetric trapezoidal compound channel. The simulations were conducted using a Computational Fluid Dynamics (CFD) code FLUENT, whereas a Reynolds Averaged Navier-Stokes (RANS) technique based on Reynolds stress model (RSM) was implemented for turbulence closure. The numerical model successfully replicated the flow behavior and showed a good agreement with the experimental data. The present study concluded the presence of quite-S shaped velocity profile in the layered vegetated floodplains when the short vegetation was submerged during high flows or floods, whereas the velocity profile was uniform or almost logarithmic during low floods or when both short and tall vegetation remained emergent. The lateral exchange of mass and momentum was promoted due to the flow separation and instability along the junction of the floodplains and main channel. The flow velocities were significantly reduced in the floodplains due to resistance offered by the vegetation, which consequently resulted in an increased percentage i.e. 67-73%, of passing discharge through the main channel. In general, the spatial distribution of mean flow and turbulence characteristics was considerably affected near the floodplain and main channel interfaces. Moreover, this study indicated a positive flow response for the sediment deposition as well as for the nourishment of the aquatic organisms in the riparian environment.

*Keywords:* Compound Channel; Vegetated Floodplains; Numerical Modelling; Flow Characteristics.

## 1. Introduction

Vegetation on flood plains is a world-wide engineering problem in most of the natural rivers, which does not only affect the flow conveyance capacity but also influences the ecological system of rivers [1]. Natural rivers are generally functioned by the main channel for conveyance of the primary flow and a vegetated floodplain to carry the extra flow during floods. The vegetation on the floodplain offers hydraulic resistance as it typically leads to the reduced flow velocity and increases the difference in velocity between the main channel and the floodplain. Many river problems demand accurate predictions of the flow conveyance in compound channels. It facilitates the engineers in the

* Corresponding author: m.ahmad201017@gmail.com

http://dx.doi.org/10.28991/cej-2020-03091513

development of important information related to the flood protection, design of hydraulic structures, and sediment load estimation to plan for effective prevention measures [2-4]. It is related to other practical engineering problems such as river training and morphology, dredging and design of flood alleviation works [5-7]. It encourages the hydraulic engineers to estimate the flood risks and to develop the mitigation schemes [8, 9].

Vegetation on the floodplains has distinct functions to understand the morpho-dynamics and flood control features of river. It includes flow reduction, streamline regulation and shoreline protection against the erosion. On the other hand, it enhances sediment deposition and causes overgrowth of the vegetation [1]. Several researchers have explored different flow patterns and discharge prediction in a vegetated compound channel [10-12]. Flow conveyance in a compound channel can be accurately determined with considering the momentum-transfer mechanism across the flow sections [13-15]. Thus, the outcomes of the previous studies identified that the flow structures in a compound channel are more complex than that in a simple channel.

The flow structure at the interface of main channel and floodplains containing vegetation becomes complex due the exchange of momentum [16, 17], which affects the overall discharge carrying capacity of the channel [18]. The vegetated floodplains play a role in sediment trapping due to larger exchange of momentum [19] and helps in channel restoration [20]. Thus, the introduction of vegetation on the floodplains illustrates the better understanding of flow hydrodynamics in compound channels.

Previous researchers have investigated the compound channel flow with focusing on constant height of the vegetation on floodplains under either emergent or submerged flow conditions, which is not as real as that in natural rivers or streams. In fact, in natural riparian environment, vegetation exists with heterogeneity i.e. short vegetation such as shrubs and grass, as well as tall vegetation such as trees [21], which experiences both emergent and submerged conditions. Although there are only a few studies on flows with an array of short and tall vegetation together [21,22] in rectangular channels; however, the complex interaction of flow in the floodplains having such kind of riparian vegetation with the main channel flow needs to be explored. Thus, these studies indicate the influence of vegetation diversity on flow structures in natural riparian environment.

During the higher floods in riparian environment or in flood plains, the short vegetation becomes submerged and tall vegetation becomes emergent which results in extra complexity of the flow structure due to shear layer formation around the top of submerged vegetation [1]. On the other hand, when the water level is small during low flows, short vegetation as well as tall vegetation remains emergent. Thus, it is necessary to consider the effects of the short and tall vegetation, which contributes an extra part of complexity in the flow patterns, to effectively replicate the riparian environment. Although understanding of the flow hydrodynamics with incorporating riparian vegetation has extensively been promoted by the previous studies, discussion is still limited within the scope of heterogeneous canopies over the floodplains.

Many of the previous researchers adopted numerical simulation techniques in order to clarify the turbulent flow structures through the vegetation in open channels. For example, Nodaoka and Yagi [23] and Su and Li [24] applied Large Eddy Simulation (LES) technique for studying the turbulent flows in open channel in the presence of vegetation. A non-linear k-epsilon ($k-\varepsilon$) model was implemented by Jahra et al. [25] to clarify the mean velocity distributions and turbulent features. Kang and Choi [26] developed a Reynolds stress model (RSM) to investigate the flow structure with and without considering the effects of vegetation. The Reynolds averaged Navier Stokes (RANS) technique was adopted by Anjum and Tanaka [27, 28] in which the turbulent flow features through heterogeneous vegetation configuration were investigated utilizing CFD code FLUENT. Souliotis and Prinos [29] numerically investigated the effects of vegetation density on the flow stability and turbulence characteristics with the help of FLUENT. Thus, the involvement of numerical investigating techniques examines the turbulent characteristics more efficiently.

Zhao et al. [30] and Yan et al. [31] experimentally studied the turbulent flow structure through submerged vegetation in an open channel; whereas the wake structure in the presence of non-submerged vegetation was investigated by Yu et al. [32]. Zhao and Huai [33] utilized LES technique to study the influence of discontinuous and submerged patches of vegetation on turbulence of flow in an open channel. Moreover, they pointed that simulating the flow structures within the vicinity of vegetation cylinders is difficult to achieve through experimental investigation. Thus, overcoming this difficulty is one of the advantages of present numerical study.

The present study is focused to numerically investigate the flow behavior in a compound channel with the floodplains containing vertically layered vegetation. The main objective of the present study is to simulate the 3D flow properties by investigating the detailed velocity distribution and turbulence characteristics under a varying condition of submergence of novel kind of layered vegetation over the floodplains. The RSM is implemented for the simulation purpose. The present study can help in understanding the hydrodynamics of flow through compound channel with vegetated floodplains, better forest management in case of floods, suitable habitat from ecological point of view, and three-dimensional (3D) flow phenomena through a complex vegetation array to better elaborate the natural processes in a riparian environment.

This paper is divided into three major sections: 1. Materials and Methods: in which governing equations of the numerical model, validation of the model, and modeling setup are presented in detail, 2. Results and Discussion: where the vertical and lateral profiles distribution, and spatial distributions of the flow and turbulent characteristics are discussed, 3. Conclusions: At the end, the major outcomes of this study are concluded.

## 2. Materials and Methods

### 2.1. Governing Equations

For the steady and incompressible open channel flow, the RANS equations for the continuity and momentum can be expressed as given in Equations 1 and 2, respectively.

*Continuity equation:*

$$\frac{\partial\langle\bar{u}_i\rangle}{\partial x_i} = 0 \tag{1}$$

*Momentum equation:*

$$\langle\bar{u}_j\rangle\frac{\partial\langle\bar{u}_i\rangle}{\partial x_j} = -\frac{1}{\rho}\frac{\partial\langle\bar{p}\rangle}{\partial x_i} + \frac{v}{\rho}\frac{\partial}{\partial x_j}\left(\frac{\partial\langle\bar{u}_i\rangle}{\partial x_j} + \frac{\partial\langle\bar{u}_j\rangle}{\partial x_i}\right) - \rho\langle\overline{u_i{}'u_j{}'}\rangle \tag{2}$$

Where $\bar{u}_i$ represent the time-averaged velocity in $x_i$ direction, $\bar{u}_j$ represent the time-averaged velocity in $x_j$ direction, $v$ represent the kinematic viscosity, $\rho$ represent the density of water, $\bar{p}$ represent the pressure, and $-\rho\langle\overline{u_i{}'u_j{}'}\rangle$ represent the Reynolds stresses.

The general form of the Reynolds stresses is expressed in Equation 3 [34]. It involves different terms characterizing the partial differential equation for the independent Reynolds stresses transport.

$$\frac{\partial R_{ij}}{\partial t} = P_{ij} + D_{ij} - \varepsilon_{ij} + \prod_{ij} + \Omega_{ij} - C_{ij} \tag{3}$$

Where $\frac{\partial R_{ij}}{\partial t}$ is the rate of Reynolds stresses, $P_{ij}$ is the production rate of Reynolds stresses, $D_{ij}$ is the stresses transport due to diffusion, $\varepsilon_{ij}$ is the rate of dissipation of stresses, $\Pi_{ij}$is the stresses transport due to turbulent pressure strain interactions, $\Omega_{ij}$ is the stresses transport due to rotation, and $C_{ij}$is the convection transport.

The production term and the diffusion terms are modelled as (Equations 4 and 5, respectively):

$$P_{ij} = -\left(R_{im}\frac{\partial\langle\bar{u}_j\rangle}{\partial x_m} + R_{jm}\frac{\partial\langle\bar{u}_i\rangle}{\partial x_m}\right) \tag{4}$$

$$D_{ij} = \frac{\partial}{\partial x_m}\left(\frac{v_t}{\sigma_k}\frac{\partial R_{ij}}{\partial x_m}\right) \tag{5}$$

Where $\sigma_k = 1.0$, and:

$$v_t = C_\mu\frac{k^2}{\varepsilon} \tag{6}$$

Where $C_\mu = 0.09$.

Equation 7 shows the modeling of dissipation rate.

$$\varepsilon_{ij} = \frac{2}{3}\varepsilon\delta_{ij} \tag{7}$$

Where $\varepsilon$ represent the dissipation rate of turbulent kinetic energy and $\delta_{ij}$ represents the Kronecker delta which is expressed as $\delta_{ij} = 1$ if $i = j$ and $\delta_{ij} = 1$ if $i \neq j$.

The rotation term is given in Equation 8.

$$\Omega_{ij} = -2\omega_k(\langle\overline{u_j{}'u_m{}'}\rangle e_{ikm} + \langle\overline{u_i{}'u_m{}'}\rangle e_{jkm}) \tag{8}$$

Where $\omega_k$ represents the rotation vector and $e_{ijk}$represents the alternating symbol; $e_{ijk} = +1$ if $i$, $j$ and $k$ are different and in cyclic order, $e_{ijk} = -1$ if $i$, $j$ and $k$ are different and in anti-cyclic order; and $e_{ijk} = 0$ if any two indices are the identical.

The pressure strain term is expressed in Equation 9.

$$\prod_{ij} = -C_1\frac{\varepsilon}{k}\left(R_{ij} - \frac{2}{3}k\delta_{ij}\right) - C_2\left(P_{ij} - \frac{2}{3}P\delta_{ij}\right) \tag{9}$$

Where $C_1 = 1.8$ and $C_2 = 0.6$

Also, the turbulent kinetic energy *"k"* is modelled in Equation 10.

$$k = \frac{1}{2}\left(\langle\overline{u_i'^2}\rangle + \langle\overline{u_j'^2}\rangle + \langle\overline{u_k'^2}\rangle\right) \quad (10)$$

And, the convective term is simply modelled in Equation 11.

$$C_{ij} = \frac{\partial(\rho\langle\overline{u}_k\rangle\langle\overline{u_i'u_j'}\rangle)}{\partial x_k} \quad (11)$$

## 2.2. Experimental Setup for Model Validation

The numerical model was validated with the experimental data of Takuya et al. [1]. They conducted a flume study in a 4.8m long and 0.8m wide channel. The test flume was adjusted to simulate a symmetric trapezoidal compound cross section with partial vegetation belt on the edges of floodplains. The bed slope was fixed to a value of 1/1000. The rigid vegetation cylinders were arranged in a staggered pattern with vegetation density ($\lambda_{veg}$) of 2 $m^{-1}$. The height ($h_v$) and diameter ($D$) of each cylinder were 6 cm and 0.6 cm, respectively. The longitudinal and transverse spacing between the cylinders was equivalent to $\Delta S$ = 5.5 cm. The discharge used in the considered case was $Q$= 10 L/s corresponding to the emergent vegetation. The experimental conditions are given in Table 1.

## 2.3. Boundary Conditions

The modeled geometry for validation was simplified to a reduced length ratio of 1/3 due to small vegetation size and large mesh. A computational domain of 1.6 m length was modeled, while all the other dimensions were kept the same as shown in Figure 1(a) (top view) and Figure 1(b) (lateral view). An unstructured mesh with tri-pave scheme was used which provided 1.4 million grid points. A periodic boundary condition was adopted at the inlet/outlet of the domain which offered an interface (translational periodicity) between the inlet and outlet of the domain. A symmetry boundary condition was used at the free surface, and a wall boundary with no-slip condition was applied at the domain bed, side walls and cylinder walls.

**Table 1. Experimental conditions (Takuya et al. 2014 [1]), where $h_f$ is the flow depth in floodplain, $h_m$ is the flow depth in the main channel, $\lambda_{veg}$ is the vegetation density, $h_v$ is the height of the cylinder, $\Delta S$ is the spacing between the vegetation cylinders, $Q$ is the discharge, $U$ is the average velocity, $F_r$ is Froude number, $R_e$ is Reynolds number for cylinder and $R_e^*$ is flow Reynolds number.**

| $h_f$ (cm) | $h_m$ (cm) | $\lambda_{veg}$ ($m^{-1}$) | D (cm) | $h_v$ (cm) | ΔS (cm) | Q (L/s) | U (m/s) | $F_r$ | $R_e$ | $R_e^*$ |
|---|---|---|---|---|---|---|---|---|---|---|
| 5.75 | 9.25 | 2.0 | 0.6 | 6 | 5.5 | 10 | 0.181 | 0.220 | 1086 | 12507 |

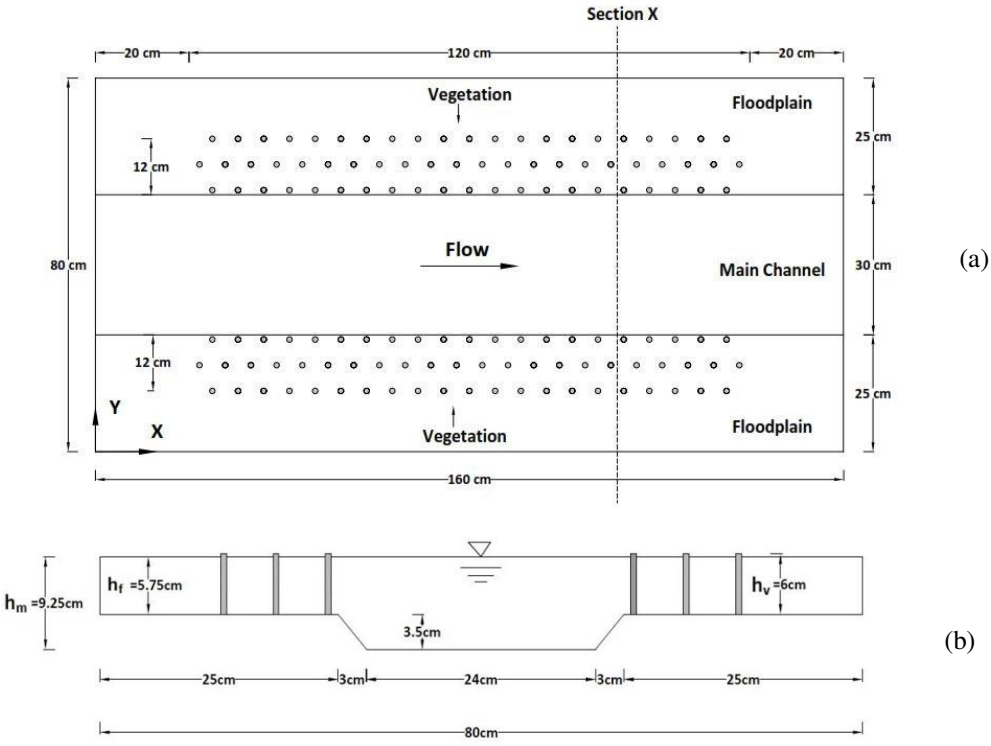


**Figure 1. Experimental scheme (Takuya et al. 2014 [1]), (a) plan view showing partly covered vegetation on floodplains, and (b) lateral view**

The numerical simulations were performed with a computational fluid dynamics (CFD) code FLUENT. The turbulence closure was achieved with a 3D RSM. The coupling between pressure and velocity was developed with the SIMPLE method. The solution was considered to be converged after all the residuals were reached to $1\times10^{-6}$. The standard wall function was applied as a near wall treatment. The nodes occurring in cross-wise and depth-wise directions were doubled to test a mesh independent trial. The variations in the results of primary velocities were less than 1% due to mesh refinement, which indicated that the mesh independent results are achieved.

## 2.4. Validation of Numerical Model

The channel cross section was considered axis-symmetric to the central vertical axis. Figures 2(a) and 2(b) shows the comparison of computational and experimental data of surface and depth averaged velocities along the cross-section X (see Figure 1a). The vertical axis shows the stream-wise velocity, whereas the horizontal axis shows the transverse distance in $y$-direction. It can be observed by both experimental and numerical results that the flow velocities are significantly reduced in the vegetation part of the floodplain i.e. 0.13 cm < $y$ < 0.25 cm (Figure 2a-b). On the contrary, the velocities are visibly higher in the non-vegetation part of the floodplain i.e. 0 cm < $y$ < 0.13 cm, as well as in the main channel i.e. 0.25 cm < $y$ < 0.40 cm. This identifies that the presence of vegetation on the edge of floodplains can offer noticeable resistance to the flow and can affect the discharge carrying capacity of the main channel.

The results show that the computational data is in close agreement with that of the experimental data, demonstrating the validity of the present numerical model. However, the computational results show a minor difference to that of experimental results in the form of slightly over estimation of the velocity values, which may be due to the error caused by the RSM simplification.

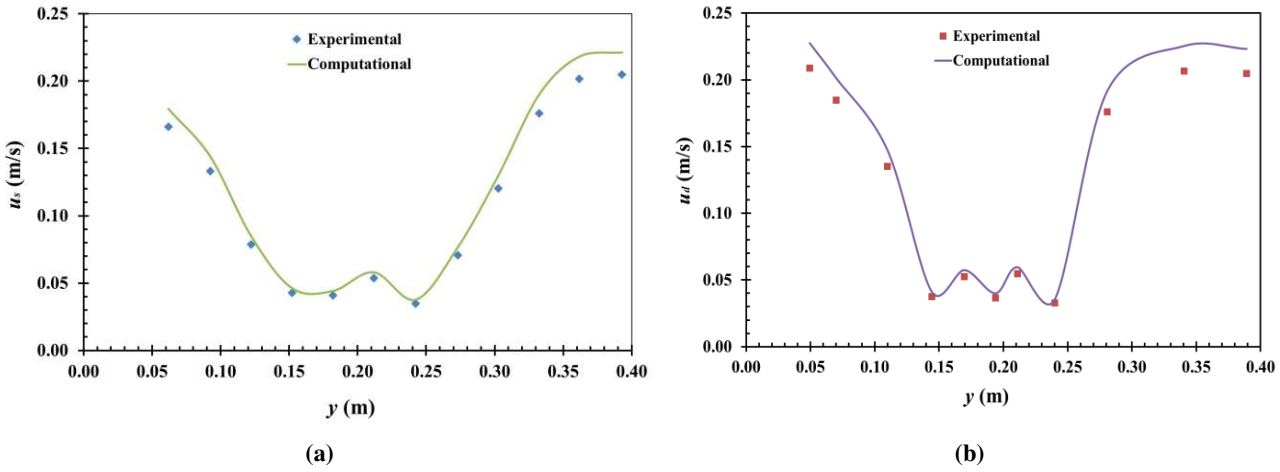


**Figure 2. Comparison of experimental and computational data of (a) surface velocity and (b) depth averaged velocity along the half width at cross section X**

## 1.1. Model Setup for Present Study

For the present study, similar dimensions of domain i.e.1.6 m long and 0.8 m wide, were considered as were used for the validation purpose. The floodplains of the compound channel were consisted of layered vegetation (short vegetation of 6cm height, and tall vegetation of 12 cm height) of same diameter i.e. $D$= 0.6 cm and spacing i.e. $\Delta S$= 5.5 cm, which covered full width of the floodplains. The scheme of the computational domain is shown in Figure 3(a). Two discharge conditions of $Q$= 10 L/s and $Q$= 18 L/s were considered in order to simulate the behavior of riparian (floodplain) vegetation of layered configuration under both emergent and submerged condition of short vegetation considering low level and high-level flood, respectively.

The lateral views of both cases configuration (Case A and Case B) are shown in Figures 3(b) and (c). All the boundary conditions for the simulations were kept same as those of validation case. The adopted unstructured mesh used for the present study gave 2.4 million grid points. The hydraulic and geometric conditions are detailed in Table 2.

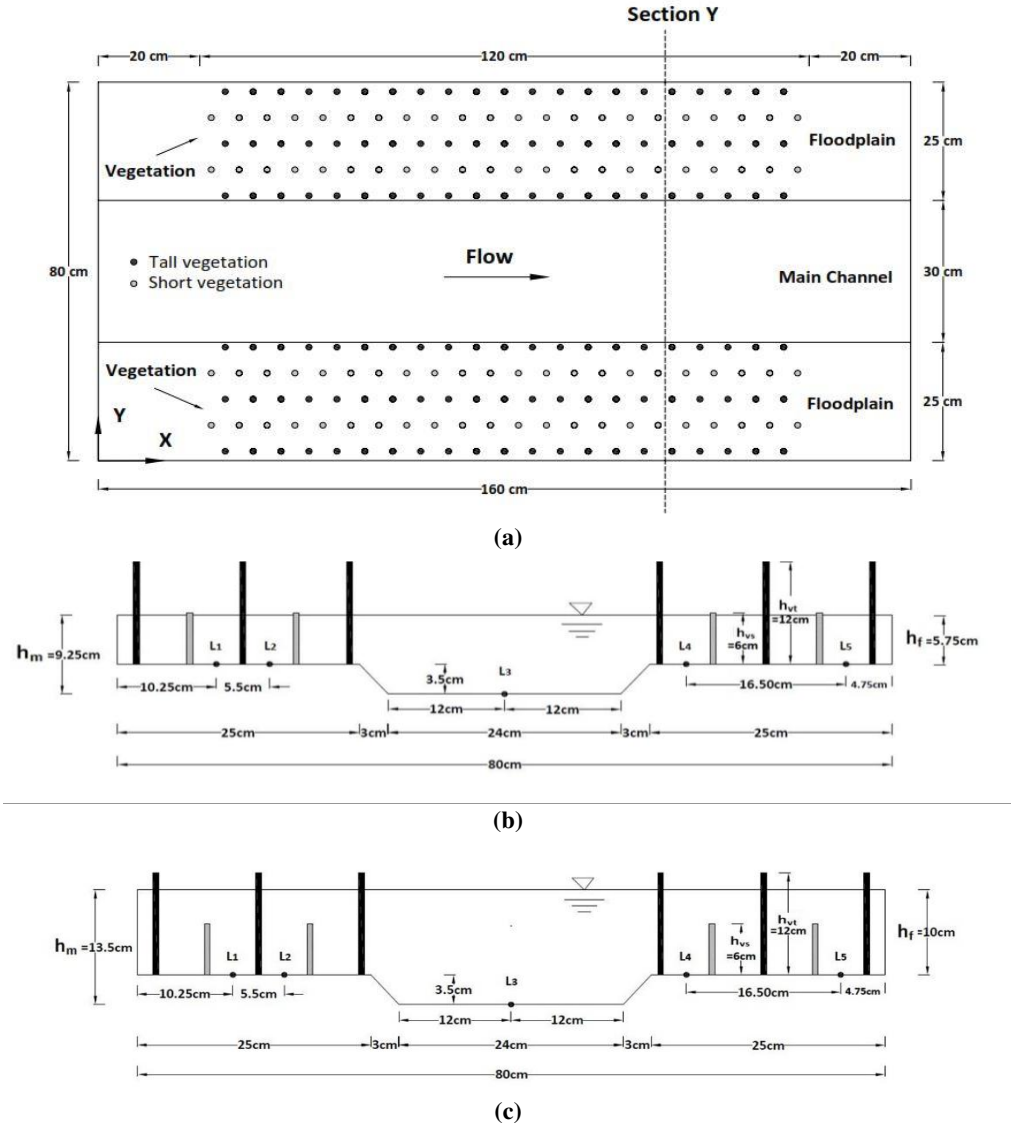


**Figure 3. Schematic diagram of computational domain, (a) plan view showing layered vegetation on floodplains, and lateral views for (b) Case A, and (c) Case B**

**Table 2. Hydraulic conditions for present study, where $h_{vs}$ is the height of short cylinder, $h_{vt}$ is the height of tall cylinder.**

| *Case* | $h_f$ (cm) | $h_m$ (cm) | $\lambda_{veg}$ ($m^{-1}$) | $D$ (cm) | $h_{vs}$ (cm) | $h_{vt}$ (cm) | $\Delta S$ (cm) | $Q$ (L/s) | $U$ (m/s) | $F_r$ | $R_e$ | $R_e^*$ |
|---|---|---|---|---|---|---|---|---|---|---|---|---|
| A | 5.75 | 9.25 | 2.0 | 0.6 | 6 | 12 | 5.5 | 10 | 0.181 | 0.220 | 1086 | 12507 |
| B | 10 | 13.5 | 2.0 | 0.6 | 6 | 12 | 5.5 | 18 | 0.202 | 0.193 | 1212 | 22503 |

For the measurement of flow characteristics, important locations ($L_1$-$L_5$) on a lateral cross section Y were adopted (see Figure 3). These locations are located in the center region of floodplains ($L_1$ and $L_2$), at the beginning and end of the floodplains ($L_4$ and $L_5$, respectively), and also in the centerline of the main channel along the width ($L_3$). These kind of important locations over a cross-section have also been investigated by Yang et al. [18]. Moreover, the flow structures have also been investigated in the form of spatial distribution of contour plots over the cross-section Y as well as over the free surface in order to further clarify the flow phenomena.

## 3. Results and Discussion

### 3.1. Flow Characteristics

#### 3.1.1. Vertical Profiles Distribution of Velocity

The vertical profiles distribution of mean stream-wise velocity at specified locations for both cases (Case A and B) is depicted in Figure 4(a-b). The horizontal axis represents the stream-wise velocity ($u$) which was made non-dimensional with respect to average velocity ($U$), whereas the vertical axis represents the depth of floodplain ($h_f$)

which was made non-dimensional with respect to short vegetation height ($h_{vs}$). It can be observed that the flow velocities in both cases are significantly reduced within the region of floodplains ($L_1$–$L_2$ and $L_4$-$L_5$); however, there is no clear difference between the velocities magnitudes measured within the floodplain regions. The velocity magnitudes are noticeably very high in the main channel region i.e. location $L_3$. This identifies that the vegetation within the floodplains of compound channel significantly affects the velocity distribution and offers resistance to the flow. This resistance caused by floodplain vegetation has also been discussed and observed in the previous studies [1, 16]. On the contrary, the velocity in the main stream region without the vegetation increases that could be a compensation of the resistance to the flow in the floodplains; thus, it can consequently result in an increase in the discharge carrying capacity of the main channel.

Although, the velocities in both cases close to the bed reduced to minimum due to the resistance offered by the domain bed; however, difference in the velocity structures exist between Case A and Case B (Figure 4a-b). The distribution of velocity in Case A remained almost constant above the bed region up-to the height of free surface at all the locations. This is due to the reason that both the short and tall vegetation were emergent in this case, where an almost constant drag to the flow was offered by the vegetation structures. This constant distribution of velocity profiles is identical to that observed by previous researchers of flow investigations through the emergent vegetation [35, 36]. On the contrary, the simulated velocity profiles in floodplains for Case B shows a different structure due to the submergence of short vegetation. The velocity distribution above the bed region remained almost constant up-to the vicinity region of shorter submerged vegetation i.e. $h_f/h_{vs} \approx 0.8$, followed by an inflection point over the top of submerged vegetation, showing consistency with the results obtained by previous studies [21, 37]. This inflection point in the velocity profiles over the top of short submerged vegetation is due to the exchange of momentum between the top of submerged vegetation and the overlying flow. The velocity gradient continued up-to the region just above the top of short vegetation height i.e. $h_f/h_{vs} \approx 1.2$, and then became constant above it until the free surface. Thus, a mixing layer over the vicinity region of shorter submerged vegetation ($h_f/h_{vs} \approx 0.8$ to $h_f/h_{vs} \approx 1.2$) is resulted. A mixing layer is produced when the canopy absorbs sufficient momentum to generate an inflection point in the velocity profile, which is required for triggering the Kelvin–Helmholtz instability. Thus, the vortices produced due to this instability dominate the mass and momentum exchange between the canopy and the overlying flow in aquatic canopies [38, 39].

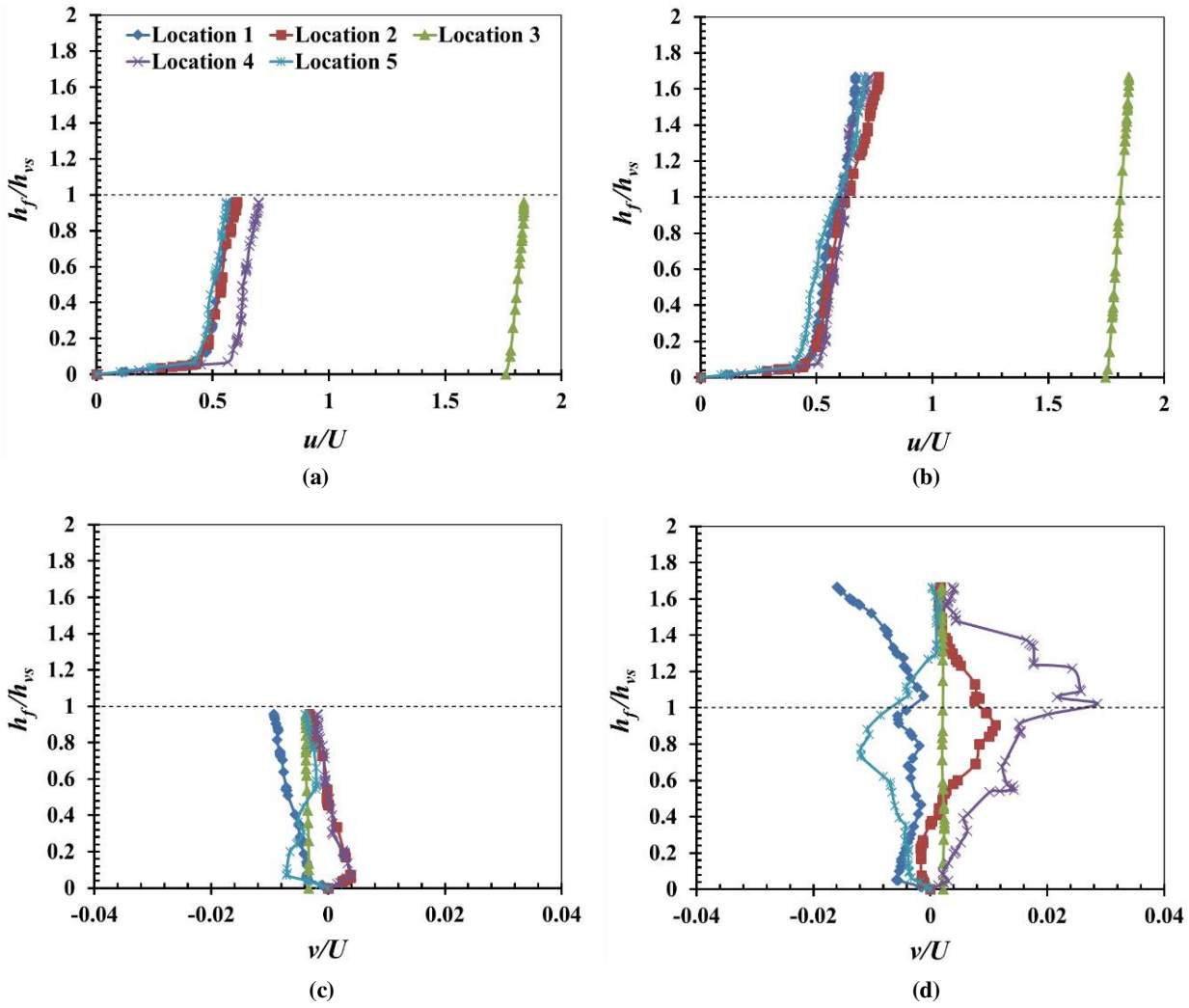

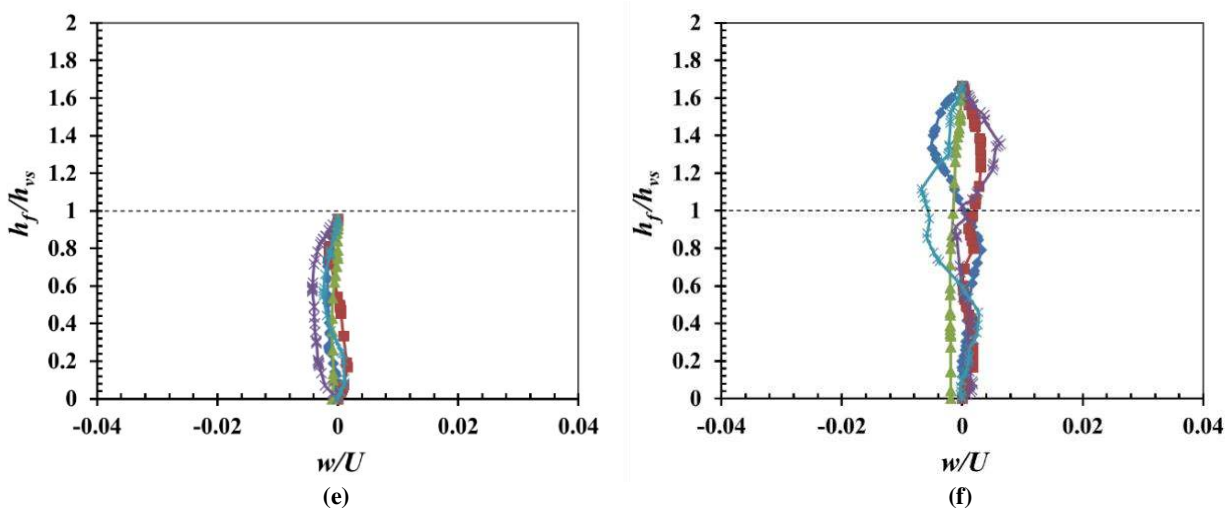


**Figure 4. Vertical profiles distribution of: streamwise velocity for (a) Case A, and (b) Case B; transverse velocity for (c) Case A, and (d) Case B; and vertical velocity for ((e) Case A, and (f) Case B. For the specified locations, see Figure 3**

Moreover, the velocity distributions followed almost *S*-shaped pattern on floodplains when short vegetation was submerged (Figure 4b). However, an almost logarithmic profile is predominantly observed in the main channel ($L_3$). These distributions are in agreement to the experimental results of Yang et al. [18]. The velocities in the overlying flow above the short vegetation height i.e. $h_f/h_{vs}>1$, are increased by a percentage difference of 18-30% due to the reason that less resistance is offered by the sparse arrangement of tall emergent vegetation in this region, as compared to the region within the height of short vegetation i.e. $h_f/h_{vs}< 1$.

The vertical profiles distribution for mean transverse velocity ($v$) and vertical velocity ($w$) for both cases is depicted in Figure 4(c-d) and Figure 4(e-f), respectively. The results show that the velocity components in the transverse and vertical directions are almost minimum i.e. close to zero, at all the locations, in comparison to that of stream-wise velocity components (Figure 4a-b). However, fluctuations in the velocity profiles are observed at the locations in the floodplains ($L_1$–$L_2$ and $L_4$-$L_5$) due to the influence of vegetation structures, whereas no fluctuations in the velocity profile at the location in the main channel ($L_1$) is observed. These fluctuations in the transverse and vertical velocities have also been observed by previous researchers [22, 27]. The fluctuations in the velocity profiles are observed to be slightly larger in the transverse direction as compared to those in the vertical directions for both cases (Case A and B). Moreover, the velocities components in the transverse and vertical directions are considerable as they indicate the secondary flow and lateral exchange of momentum.

### 3.1.2. Spatial Distribution of Velocity

The contour plots distribution of mean stream-wise velocity over the cross-section Y is presented in Figure 5(a-b). It can be noticed that the velocities are reduced to minimum close to bed due to the resistance offered by it. A clear difference between the floodplains and main channel regions can be observed. The flow in the main channel i.e. 25 cm < $y$ < 55 cm, experienced larger velocities, where the maximum values of velocity were observed to be in the center region of the main channel i.e. $y \approx 40$ cm. At the interface between the main channel and the floodplain regions i.e. $y \approx$ 25 cm and i.e. $y \approx 55$ cm, the flow instability in the lateral direction is triggered by the flow shear due to the presence of vegetation over the floodplains, which results in the formation of coherent vortices and exchange of momentum [40, 41]. The velocities in the floodplain regions are significantly reduced due to the drag offered by the vegetation. Thus, large exchange of momentum from the main channel (having high velocity) to the floodplains (having low velocities) is expected to occur. Moreover, these low velocity regions could significantly encourage the deposition of sediments in the vegetated floodplains. Within the floodplain regions, a vertical mixing layer is also observed in Case B (Figure 5b) over the region of short submerged vegetation due to the vertical exchange of momentum over this region of flow, showing consistency with the results observed in Figure 4b. However, the velocity distribution is almost constant in Case A (Figure 5a) where the vegetation canopy is emergent.

Figure 5(c-d) depicts the spatial distribution of flow velocity over the free surface for both cases. The discharge passing through the main channel can be easily differentiated from the discharge passing through the vegetated floodplains. The velocity rapidly increased from the vegetated floodplain regions to the main channel region, followed by a significant transition and inflection along the interface between these regions. Then, coherent vortices resulted due to the flow instability dominate the lateral exchange of mass and momentum between the main channel and vegetated floodplain regions [42, 43]. Moreover, the velocities are reduced to minimum in the regions directly downstream of the vegetation structures, followed by vortices and wakes i.e. primary Karman vortex streets, which disappeared after travelling some distance behind the individual vegetation structures. The flow velocities failed to

recover their normal patterns as the influence of vegetation remains for a specific distance behind the downstream edge. From ecological point of view, aquatic organisms find these regions of low flow velocity suitable for their physical environment and growth [44, 45]. Sediment deposition also occurs in these regions. Previous researchers also pointed out that the wake regions behind the vegetation are the regions of fine particle deposition that promote further growth of the vegetated region [46, 47].

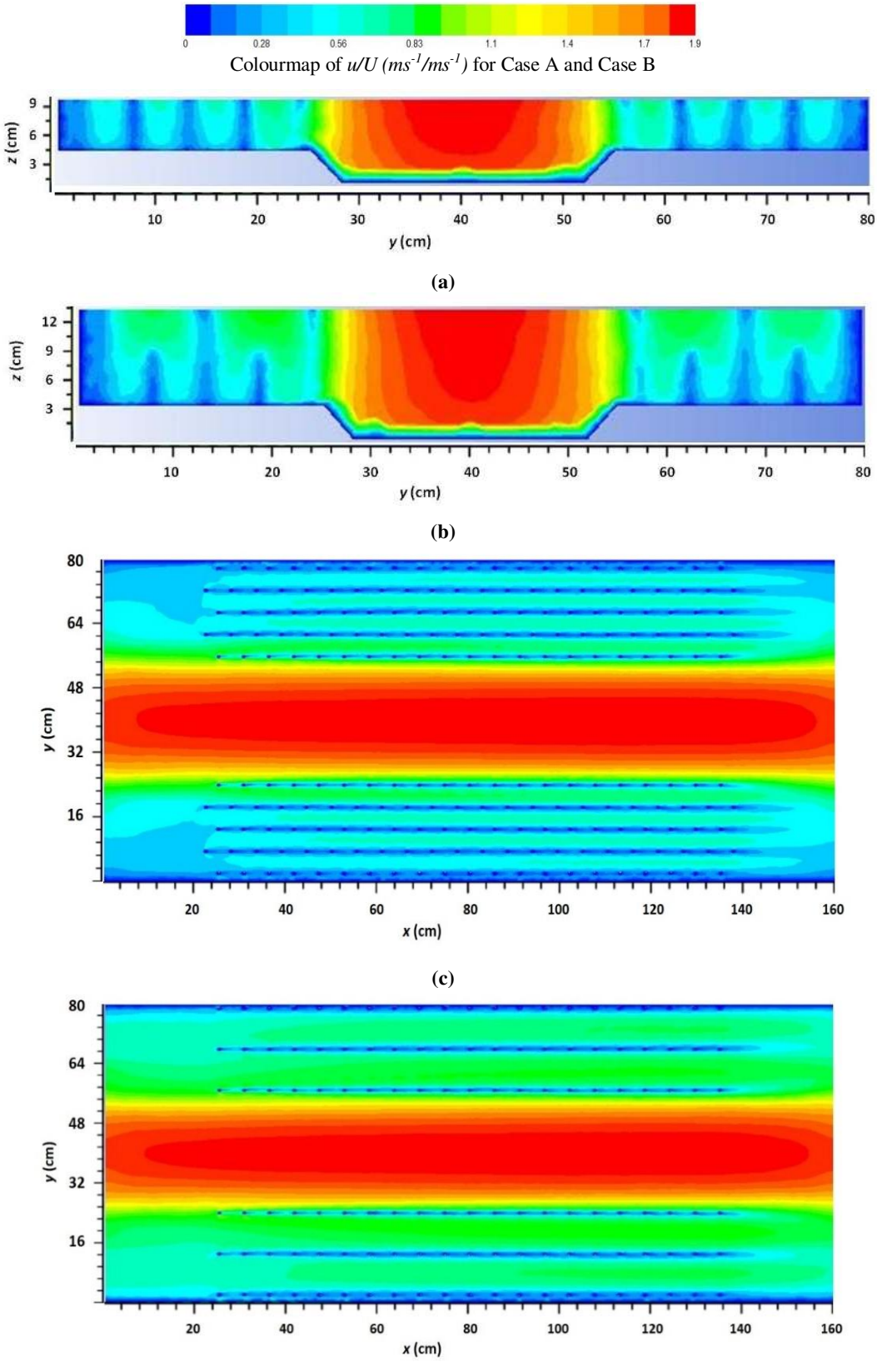


**Figure 5. Spatial distribution of mean stream-wise velocity (*u/U*) over cross-section Y for (a) Case A, and (b) Case B; and over free surface for (c) Case A, and (d) Case B. For the cross-section Y, see Figure 3a**

### 3.1.3. Lateral Profile Distribution of Velocity

The variations of the depth averaged mean stream-wise velocity along half of the cross-section Y (due to symmetry) is depicted in Figure 6. The data for both cases further clarifies that the main channel without vegetation i.e. 25 cm < $y$ < 40 cm, has higher flow velocities compared with the vegetated floodplain region i.e. 0 cm < $y$ < 25 cm, identifying the effect of vegetation and resistance due to it. Within the floodplain region, rise and fall in flow velocities can be observed, which is due to the influence of the vegetation; where slightly higher velocities are present in adjacent regions of vegetation structures and comparatively lower velocities occurred in the regions directly downstream of vegetation, as can be observed in Figure 5. Along the interface (represented by a dashed line), a strong rise in depth averaged velocity can be observed while moving from floodplain region to the main channel region, resembling the compensation of higher flow resistance due to vegetation in the floodplain. A remarkable velocity difference is noticed between the main channel and vegetated floodplain. The discharge (calculated through the velocity data) passing through main channel of the compound section increased by a percentage difference of 73% and 67% for Case A and Case B, respectively, as compared to the discharge through the floodplains, which favors the increasing conveyance capacity of compound or natural river channels in severe flood conditions. Moreover, the depth averaged flow velocities are also observed to be slightly higher i.e. 9% larger, in the floodplain region for Case B, as compared to that of Case A. This may be due to the reason of higher initial flow velocity or reduction of the drag by the sparse arrangement of tall emergent vegetation in Case B.

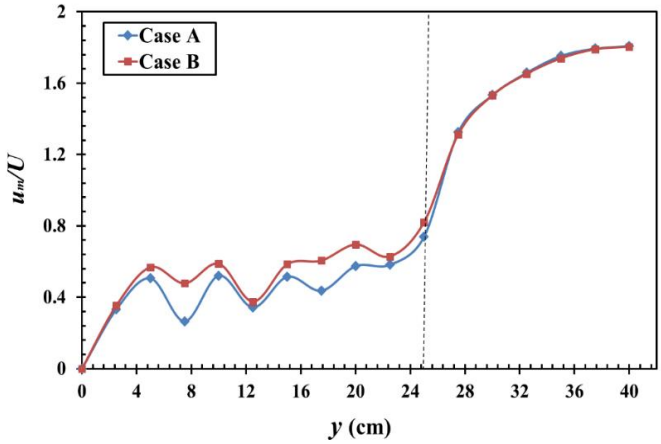


**Figure 6. Variations of depth averaged mean velocity ($u_m/U$) along the cross-section Y**

## 3.2. Turbulent Characteristics

### 3.2.1. Vertical Profiles Distribution of Reynolds Stress

Reynolds stresses (that are used to represent turbulence characteristics) including normal stresses *(u'u', v'v', w'w')* and shear stress *(-u'w')* measured at specified locations are presented in Figure 7(a-h) for both cases (Case A and B). All the stresses were made dimension-less with respect to $U^2$. In Figure 7(a-h), *u'* indicates the velocity fluctuations in streamwise direction, *v'* indicates the velocity fluctuations in transverse direction, and *w'* indicates the velocity fluctuations in vertical directions. Larger values of Reynolds stresses accumulated close to the bed region for both cases, showing consistency with those observed in the previous research work by Anjum et al. [22]. Whereas, while moving above the bed region, the Reynolds stress distribution became uniform at almost all the locations.

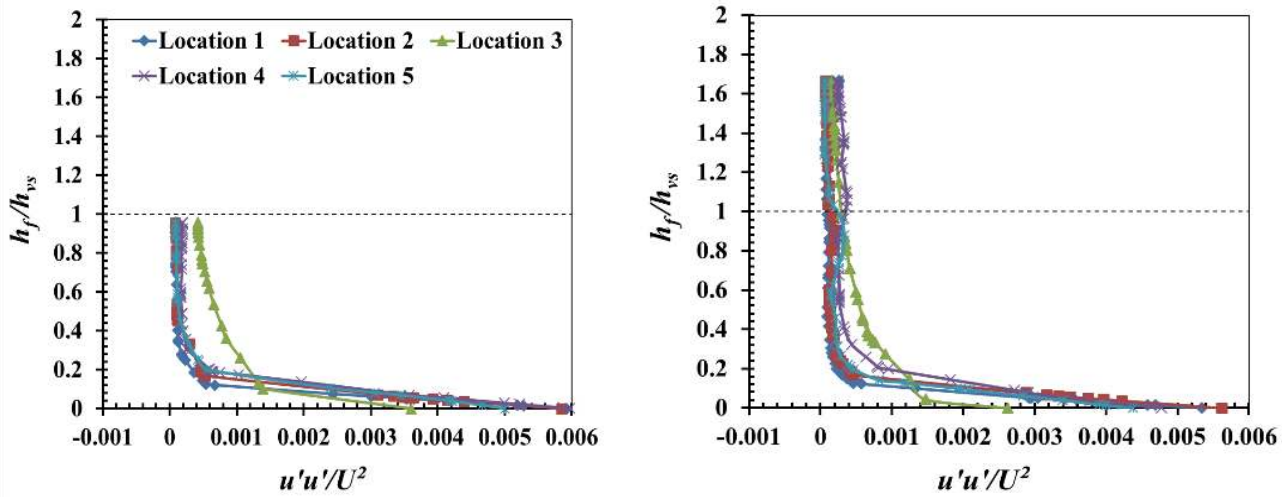

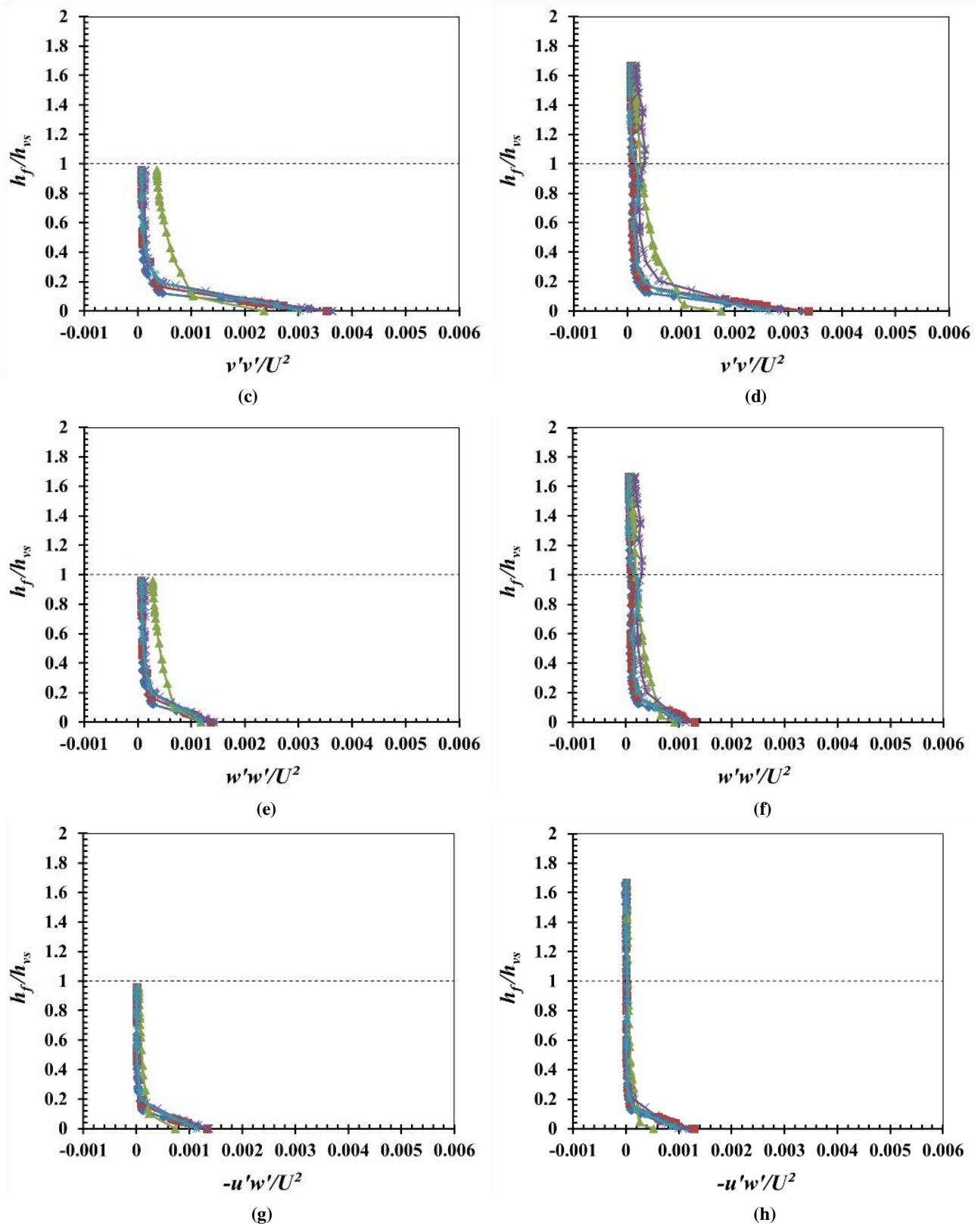


**Figure 7. Vertical profiles distribution of Reynolds normal stresses (*u'u', v'v', and w'w'*) for (a,c,e) Case A, (b,d,f) Case B, and Reynolds shear stress (*-u'w'*) for (g) Case A, and (h) Case B**

Moreover; in case B, a slight modulation in the Reynolds stress profiles around the mixing layer region i.e. $0.8 < h_f/h_{vs} < 1.2$, is observed for the locations in floodplain regions ($L_1$-$L_2$ and $L_4$-$L_5$). However, the distribution of stresses again became constant above the mixing layer region i.e. $h_f/h_{vs} > 1.2$. The results also show slightly less accumulation of Reynolds shear stress close to the bed region (Figure 7g-h), as compared to other Reynolds normal stresses (Figure 7a-f). In addition to this, the bed region acquires high Reynolds stresses in the floodplain regions ($L_1$-$L_2$ and $L_4$-$L_5$), as compared to the main channel region ($L_3$). The sharp spatial variation in the Reynolds stress influences the dynamics

of sediments, which affects the particle size distribution of the sediments available in the flow. Thus, these regions of influenced Reynolds stresses near the bed could encourage the deposition of sediments in the canopy regions [33].

### 3.2.2. Lateral Profile Distribution of Turbulent Kinetic Energy

The variation in the dimensionless depth-averaged Turbulent Kinetic Energy (*TKE*, Figure 8) along the cross-section Y further depicts the difference of turbulent flow structure between the vegetated floodplain and main channel without the vegetation. Within the vegetation region of floodplains, fluctuations in the depth-averaged *TKE* can be observed, followed by a saw-tooth dissemination, which showed consistency with the previous research works [33, 48]. Along the interface of floodplain and main channel i.e. $y \approx 25$ cm, for both cases (Case A and B), a peak in the *TKE* is observed due to the interaction of slow and fast flow over this region which caused a larger turbulence. On the contrary, the distribution of *TKE* is observed to be uniform in the main channel region. This identifies the existence of turbulence more on the vegetated region of floodplains as compared to the main channel region. The production of depth-averaged *TKE* is also found to be slightly higher for Case A due to the larger hindrance offered by the overall emergent canopy, as compared to that in Case B.

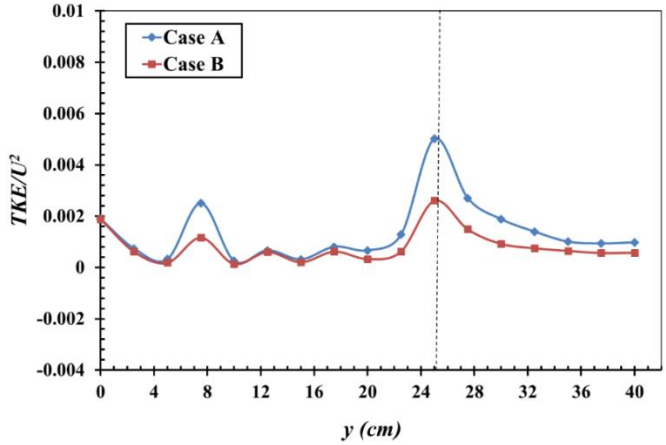


**Figure 8. Variations of depth averaged turbulent kinetic energy (*TKE*)along the cross-section Y.**

### 3.2.3. Vertical Profiles Distribution of Turbulent Intensity

Figure 9 (a-b) shows the turbulent intensity (%) profiles at the specified locations for all the cases. It can be witnessed that the percentage of turbulence is highest close to the bed region at almost all the locations for Case A and Case B. Along the depth of flow above the bed region, the intensity percentage decreased logarithmically at location $L_3$ as no resistance due to the vegetation was observed in the main channel. On the contrary, the vertical distribution of turbulent intensity at other locations ($L_1$–$L_2$ and $L_4$-$L_5$) remained almost uniform along the flow depth within the height of short vegetation i.e. $h_f/h_{vs} < 1$, for both cases (Case A and B). Moreover, a slight inflection in the intensity profiles for the locations in the floodplains ($L_1$–$L_2$ and $L_4$-$L_5$) is observed around the top of shorter submerged vegetation i.e. $h_f/h_{vs} \approx 1$, for Case B (Figure 9b), which is due to the variation of vegetation density and drag offered by it. This shows consistency with those profiles of velocity in Figure 4b. Furthermore, the turbulent intensity at locations in the floodplains ($L_1$–$L_2$ and $L_4$-$L_5$) is more influenced by vertically layered vegetation as compared to the location $L_3$ in the main channel.

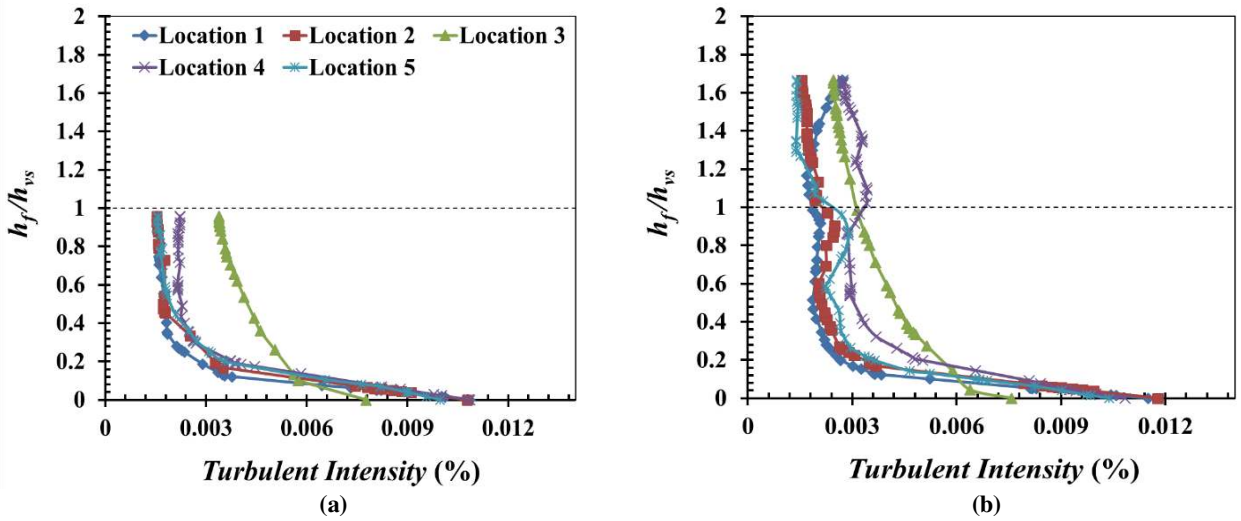


**Figure 9. Vertical profiles distribution of turbulent intensity (%) for (a) Case A, and (b) Case B**

### 3.2.4. Spatial Distribution of Turbulent Intensity

Spatial distribution of turbulent intensity is reported here to study the turbulence in the compound channel with layered vegetated floodplains. Figure 10(a-b) shows the contour plots of turbulent intensity for all the cases (A–B) along the cross-section Y. The spatial variation of the intensity distribution is high in the vegetated floodplains, indicating that the flow structure is non-uniform in these regions. Thus, larger percentage of turbulence is observed in the floodplain regions, which is due to the presence of vegetation. Within the region of above the short vegetation height for Case B (Figure 10b), the percentage of turbulence significantly decreased due to the reduction in drag by the vegetation. A clear difference is observed between the floodplain regions and the main channel region. Close to the bed region of main channel, the amount of percentage is also observed to sufficiently increase due to the resistance offered by the bed, showing correspondence to the low velocity observed in Figure 5(a-b). Moreover, the intensity in the main channel tries to achieve a uniform distribution above the bed region. Along the interface of the main channel and floodplains, a strong turbulence in the flow can be observed which is due to the reason of flow instability and exchange of momentum over this region of flow.

To further clarify the turbulent flow structure in the compound channel, contour plots of intensity over the free surface have been plotted and presented here (Figure 10c-d). It further shows the influence of layered vegetated floodplains on the flow turbulence. Higher percentage of turbulent intensity is observed directly behind the vegetation cylinders in both cases (Case A and B) due to high flow resistance in these regions, followed by trailing vortices which requires some sufficient distance to reach in the stable state. A stronger rise in the flow turbulence over the interface region of floodplains and main channel is found, followed by a decrement in the turbulence percentage while moving away from the floodplains towards the main channel. This effect on the interface region of floodplains and main channel has also been studied in the previous researches [16, 18]. This signifies the promotion of lateral exchange of momentum at the boundary of main channel and floodplains. This kind of complex flow structure around the vegetation vicinity and interface of both regions is difficult to capture in an experimental study [33, 49]. Thus, it demonstrates the significant advantage of present numerical study. Moreover, due to high initial flow velocity and Reynolds number, the overall turbulent intensity in Case B is found to be higher i.e. 20%, as compared to that of Case A.

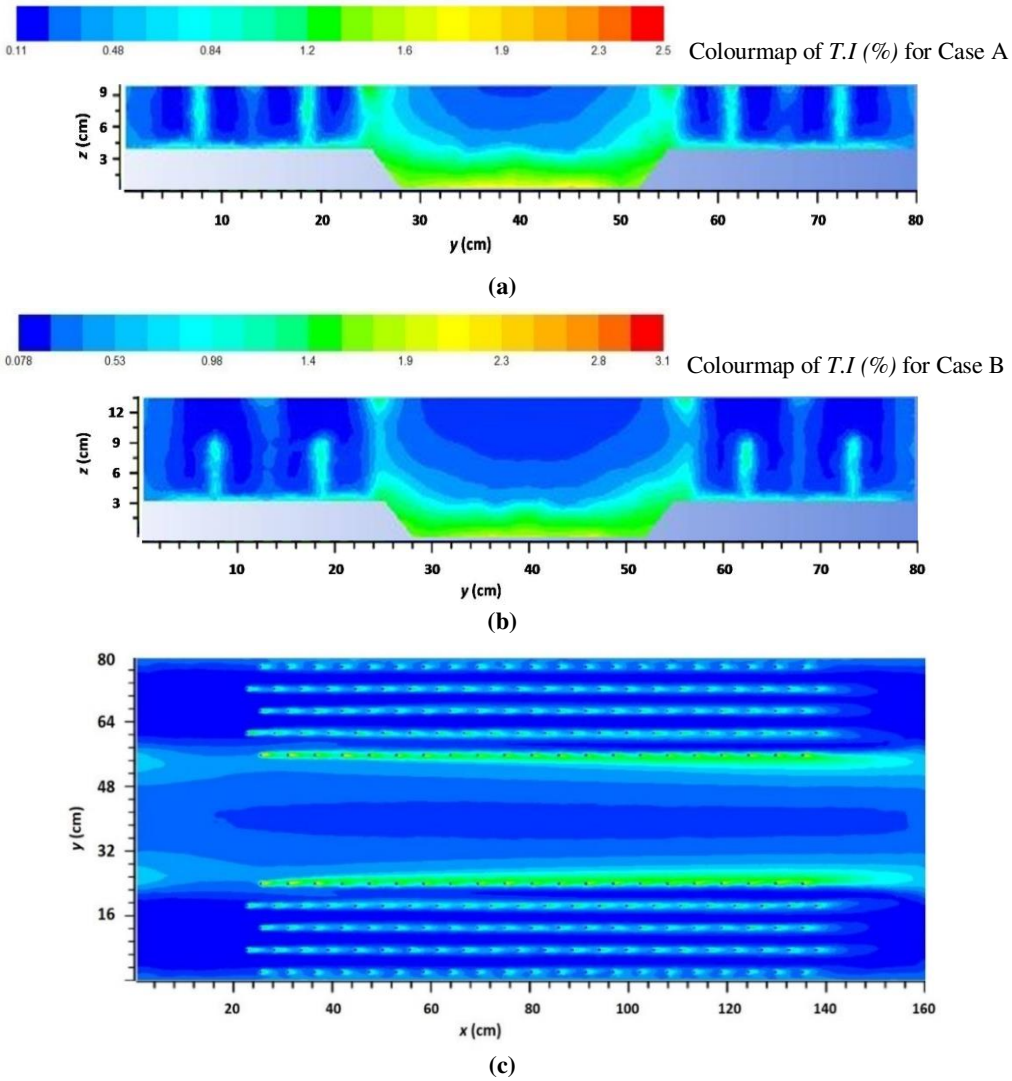

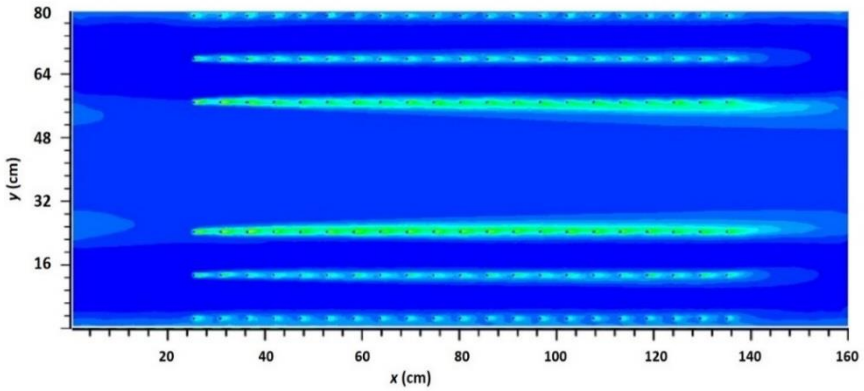


**(d)**

**Figure 10. Spatial distribution of turbulent intensity (%) over cross-section Y for (a) Case A, and (b) Case B; and over free surface for (c) Case A, and (d) Case B**

## 4. Conclusions

The present numerical study investigated the impact of vegetation on the compound channel to clarify the velocity distribution and turbulence characteristics over the floodplains with layered vegetation configuration. To achieve the desired objectives and computing the flow structures through vegetated compound channel, a CFD code FLUENT was used for simulation and RSM model was used for the turbulence closure. The following conclusions were drawn from the current study:

- When the short vegetation became submerged during high flows, an inflection point in the velocity distribution occurred resulting in a significant mixing layer over the top of submerged vegetation due to the vertical exchange of momentum between the top of submerged canopy and the overlying flow. Whereas, when both the short and tall vegetation remained emergent during low flows, the mean flow characteristics showed almost uniform distribution along the depth of flow.
- The flow velocities significantly reduced in the floodplain region due to the drag offered by the layered vegetation. On the contrary, the velocities as well as the discharge carrying capacity of the main channel increased by a percentage difference of 67-73%. A flow separation followed by a lateral exchange of momentum resulted along the interfacial region of vegetated floodplains and the main channel.
- The Reynolds stress distribution and turbulent intensity showed almost uniform distribution above the bed region up-to the vicinity of top of short vegetation height, followed by a slight inflection point over the mixing layer region. Moreover, a uniform distribution of Reynolds stress and low accumulation of turbulent intensity in the floodplain regions indicated a positive response for the sediment deposition as well as for the nourishment of the aquatic organisms in the riparian environment.
- The peak values of turbulent kinetic energy and turbulent intensity occurred over the interfacial region of floodplains and the main channel, signifying a strong turbulence over this region due to high instability of the flow that could promote lateral exchange of momentum over the boundary.

The present numerical study successfully replicated 3D flow behavior through a vegetated compound channel. It can help in understanding the resistance offered by the vegetation over the floodplains and give a clear understanding of the discharge carrying capacity of the compound channels. The flow hydrodynamics explored through this research could be implemented to natural riparian environment. The knowledge of resistance due to vegetation drag can help in designing effective measures to reduce the shear force that acts on bed sediment particle, structural analysis and depreciation on the land characteristics. Furthermore, the vegetation resistance over interfacial region will also significantly affect the momentum exchange and it can help in preventing inundation if applied wisely. Thus, a proper management and wise use of the vegetation would provide us a new strategy of sustainable flood protection. In addition, this study can be used to enhance our knowledge of vegetation patterns for future planning of flood protection measures and the outcomes of this study may become useful while designing ecological habitats.

More study to investigate the effect of vegetation density and varying heights of vegetation over the floodplain is required to further clarify the phenomena. In the future, the flow and turbulent characteristics for several other patterns of rigid vegetation on floodplains are required to be studied to better understand the natural environment such as natural streams and rivers.

## 5. Conflicts of Interest

The authors declare no conflict of interest.

## 3. References

[1] Takuya, U., Keiichi, K., and Kohji, M. "Experimental and numerical study on hydrodynamics of riparian vegetation". J. Hydrodyn, 26, (October 2014): 796-806. doi: 10.1016/S1001-6058(14)60088-3.

[2] Bousmar, D., and Zech, Y. "Momentum transfer for practical flow computation in compound channels". J. Hydraul. Eng, 125, (July 1999): 696-706. doi: 10.1061/(ASCE)0733-9429(1999)125:7(696).

[3] Unal, B., Mamak, M., Seckin, G., and Cobaner, M. "Comparison of an ANN approach with 1D and 2D methods for estimating discharge capacity of straight compound channels". Adv. Eng. Software, 41, (February 2010): 120-129. doi: 10.1016/j.advengsoft.2009.10.002.

[4] Martin, L.A., and Myers, W.R.C. "Measurement of overbank flow in a compound river channel". Proc. Instn. Civ. Engrs, (September 1993). doi:10.1680/iwtme.1993.24584.

[5] Ervine, D.A., Babaeyan-Koopaei, K., and Sellin, R.H.J. "Two-dimensional solution for straight and meandering overbank flows". J. Hydraul. Eng, 126, (September 2000): 653-669. doi: 10.1061/(ASCE)0733-9429(2000)126:9(653).

[6] Sahu, M., Khatua, K.K., and Mahapatra, S.S. "A neural network approach for prediction of discharge in straight compound open channel flow". Flow Measure Instrum, 22, (2011): 438-446. doi: 10.1016/j.flowmeasinst.2011.06.009.

[7] Knight, D.W., and Brown, F.A. "Resistance studies of overbank flow in rivers with sediment using the flood channel". J. Hydraulic Res, 39, (December 2001): 283-301. doi: 10.1080/00221680109499832.

[8] Kisi, O., and Cigizoglu, H.K. "Comparison of different ANN techniques in river flow prediction". Civil Eng. Environ. Syst, 24, (August 2007): 211-231. doi: 10.1080/10286600600888565.

[9] Al-Khatib, I.A., Abu-Hassan, H.M., and Abaza, K.A. "Development of empirical regression-based models for predicting mean velocities in asymmetric compound channels". Flow Measure Instrum, 33, (October 2013): 77-87. doi: 10.1016/j.flowmeasinst.2013.04.013.

[10] Pasche, E., and Rouve, G. "Overbank flow with vegetatively roughened flood plains". J. Hydraul. Eng, 11, (September 1985): 1262-1278. doi: 10.1061/(ASCE)0733-9429(1985)111:9(1262).

[11] Rameshwaran, P., and Shiono, K. "Quasi Two-Dimensional Model for Straight Overbank Flows Through Emergent". J.Hydraul. Res, 45, (2007): 302-315. doi: 10.1080/00221686.2007.9521765.

[12] Sun, X., and Shiono, K. "Flow Resistance of One-Line Emergent Vegetation along the Floodplain Edge of a Compound Open Channel". Journal of Adv. Water Resour, 32, (March 2009): 430-438. doi: 10.1016/j.advwatres.2008.12.004.

[13] Carling, P.A., Cao, Z., and Holland, et al. "Turbulent flow across a natural compound channel". Water Resour. Res, 38, (December 2002). doi: 10.1029/2001WR000902.

[14] Van Prooijen, B.C., Battjes, J.A., and Uijttewaal, W.S.J. "Momentum exchange in straight uniform compound channel flow".J.Hydraul. Eng, 131, (March 2005): 175-183. doi: 10.1061/(ASCE)0733-9429(2005)131:3(175).

[15] Pradhan, S., and Khatua, K.K. "An Improved Approach for Flow Prediction in Compound Open Channel Flow of Uniform Roughness". International Conference on Hydraulics, Water Resources, Coastal and Environmental Engineering, MANIT Bhopal, (2014).

[16] Koftis, T., and Prinos, P. "Reynolds stress modelling of flow in compound channels with vegetated floodplains". J. Appl. Water Eng. Res, (July 2016). doi: 10.1080/23249676.2016.1209437.

[17] Anjum, N., and Tanaka, N. "Hydrodynamics of longitudinally discontinuous, vertically double layered and partially covered rigid vegetation patches in open channel flow". River Res. Appl, 36, no. 1 (November 2019). doi: 10.1002/rra.3546.

[18] Yang, K., Cao, S., and Knight, D.W. "Flow Patterns in Compound Channels with Vegetated Floodplains". J. Hydraul. Eng, 133, (February 2007). doi: 10.1061/(ASCE)0733-9429(2007)133:2(148).

[19] Juez, C., Hassan, M.A., and Franca, M.J. "The origin of fine sediment determines the observations of suspended sediment fluxes under unsteady flow conditions". Water Resour. Res, 54, (July 2018): 5654-5669. doi: 10.1029/2018WR022982.

[20] Juez, C., Thalmann, M., Schleiss, A.J., and Franca, M.J. "Morphological resilience to flow fluctuations of fine sediment deposits in bank lateral cavities". Adv. Water Resour, 115, (May 2018): 44-59. doi: 10.1016/j.advwatres.2018.03.004.

[21] Liu, D., Diplas, P., Hodges, C.C., and Fairbanks, J.D. "Hydrodynamics of flow through double layer rigid vegetation". Geomorphology, 116, (April 2010): 286–296. doi: 10.1016/j.geomorph.2009.11.024.

[22] Anjum, N., Ghani, U., Pasha, G.A., Latif, A., Sultan, T., and Ali, S. "To investigate the flow structure of discontinuous vegetation patches of two vertically different layers in an open channel". Water, 10, (January 2018). doi: 10.3390/w10010075.

[23] Nadaoka, K., and Yagi, H. "Shallow-water turbulence modeling and horizontal large-eddy computation of river flow". J. Hydraul. Eng, 124, (May 1998): 493-500. doi: 10.1061/(ASCE)0733-9429(1998)124:5(493).

[24] Su, X., and Li, C.W. "Large Eddy simulation of free surface turbulent flow in partly vegetated open channels". Int. J. Numer. Methods Fluids, 39, (July 2002): 919-937. doi: 10.1002/fld.352.

[25] Jahra, F., Kawahara, Y., Hasegawa, F., and Yamamoto, H. "Flow–vegetation interaction in a compound open channel with emergent vegetation". Int. J. River Basin Manage, 9, (December 2011): 247-256. doi: 10.1080/15715124.2011.642379.

[26] Kang, H., and Choi, S.K. "Turbulence modeling of compound open-channel flows with and without vegetation on the floodplain using the Reynolds stress model". Adv. Water Resour, 29, (November 2006): 1650-1664. doi: 10.1016/j.advwatres.2005.12.004.

[27] Anjum, N., and Tanaka, N. "Study on the flow structure around discontinued vertically layered vegetation in an open channel". J. Hydrodyn, (April 2019). doi: 10.1007/s42241-019-0040-2.

[28] Anjum, N., and Tanaka, N. "Numerical modeling of the turbulent flow structure through vertically double layer vegetation". J JpSoc Civil Eng, Ser. B1(Hydraulic Engineering), 75, (2019): 487-492.

[29] Souliotis, D., and Prinos, P. "Effect of a vegetation patch on turbulent channel flow". J. Hydraul. Res, 49, (May 2011): 157–167. doi: 10.1080/00221686.2011.557258.

[30] Zhao, H., Yan, J., Yuan, S., Liu, J., and Zheng, J. "Effects of Submerged Vegetation Density on Turbulent Flow Characteristics in an Open Channel". Water, 11, (October 2019): 2154. doi: 10.3390/w11102154.

[31] Yan, P., Tian, Y., Lei, X., Fu, Q., Li, T., and Li, J. "Effect of the Number of Leaves in Submerged Aquatic Plants on Stream Flow Dynamics". Water, 11, (2019): 1448. doi: 10.3390/w11071448.

[32] Yu, Z., Wang, D., and Liu, X. "Impact of Vegetation Density on the Wake Structure". Water, 11, (July 2019): 1266. doi: 10.3390/w11061266.

[33] Zhao, F., and Huai, W. "Hydrodynamics of discontinuous rigid submerged vegetation patches in open-channel flow". J Hydro-Environ. Res, 12, (September 2016): 148–160. doi: 10.1016/j.jher.2016.05.004.

[34] Versteeg, H.K., and Malalasekera, W. "An introduction to computational fluid dynamics, The finite volume method". 2nd edition, Pearson Education Publishers, London, (2007).

[35] Tsujimoto, T., Shimizu, Y., Kitamura, T., and Okada, T. "Turbulent open-channel flow over bed covered by rigid vegetation". J. Hydrosci. Hydraul. Eng, 10, (1992): 13–25.

[36] Nepf, H.M., and Vivoni, E.R. "Flow structure in depth-limited, vegetated flow". J. Geophys. Res, 105, (December 2000): 547–557. doi: 10.1029/2000JC900145.

[37] Anjum, N., and Tanaka, N. "Experimental study on flow analysis and energy loss around discontinued vertically layered vegetation". Environ Fluid Mech, (November 2019). doi: 10.1007/s10652-019-09723-8.

[38] Finnigan, J. "Turbulence in plant canopies". Ann. Rev. Fluid Mech, 32, (January 2000): 519–571. doi: 10.1146/annurev.fluid.32.1.519.

[39] Ghisalberti, M., and Nepf, H. "The structure of the shear layer in flows over rigid and flexible canopies". Environ. Fluid Mech, 6, (June 2006): 277–301. doi: 10.1007/s10652-006-0002-4.

[40] Huai, W., Zhang, J., Wang, W. J., and Katul, G.G. "Turbulence structure in open channel flow with partially covered artificial emergent vegetation". J. Hydrol, 573, (June 2019): 180–193. doi: 10.1016/j.jhydrol.2019.03.071.

[41] Tang, X., Rahimi, H., Singh, P., Wei, Z., Wang, Y., Zhao, Y., and Lu, Q. "Experimental study of open-channel flow with partial double-layered vegetation". The 1st international symposium on water resource and environmental management (WREM 2018), Kunming, China, Volume 81, (2019).

[42] Yan, X.F., Wai, W.G.O., and Li, C.W. "Characteristics of flow structure of free-surface flow in a partly obstructed open channel with vegetation patch". Environ. Fluid Mech, 16, (April 2016): 807-832. doi: 10.1007/s10652-016-9453-4.

[43] Caroppi, G., Vastila, K., Jarvela, J., Rowinski, P.M., and Giugni, M. "Turbulence at water-vegetation interface in open channel flow: Experiments with natural-like plants". Adv. Water Resour, 127, (December 2019): 180-191. doi: 10.1016/j.advwatres.2019.03.013.

[44] Folkard, A.M., and Gascoigne, J.C. "Hydrodynamics of discontinuous mussel beds: Laboratory flume simulations". J. Sea Res, 62, (November 2009): 250-257. doi: 10.1016/j.seares.2009.06.001.

[45] Widdows, J., and Navarro, J.M. "Influence of current speed on clearance rate, algal cell depletion in the water column and resuspension of biodeposits of cockles (Cerastodermaedule)". J. Exp. Mar. Biol. Ecol, 343, (March 2007): 44-51. doi: 10.1016/j.jembe.2006.11.011.

[46] Tsujimoto, Tetsuro. "Fluvial Processes in Streams with Vegetation." Journal of Hydraulic Research 37, no. 6 (November 1999): 789–803. doi:10.1080/00221689909498512.

[47] Gurnell, A.M., Thompson, K., Goodson, J., and Moggridge, H. "Propagule deposition along river margins: Liking hydrology and ecology". J. Ecol, 96, (February 2008): 553-565. doi: 10.1111/j.1365-2745.2008.01358.x.

[48] Ghani, U., Anjum, N., Pasha, G.A., and Ahmad, M. "Numerical investigation of the flow characteristics through discontinuous and layered vegetation patches of finite width in an open channel". Environ. Fluid Mech, 19, (April 2019): 1469-1495. doi: 10.1007/s10652-019-09669-x.

[49] Anjum, N., and Tanaka, N. "Numerical investigation of velocity distribution of turbulent flow through vertically double-layered vegetation". Water Sci. Eng, 12, no. 4 (December 2019). doi: 10.1016/j.wse.2019.11.001.